Influence of Er on microstructural and dielectric properties of CaCu3Ti4O12

Article *in* Journal of Materials Science Materials in Electronics · January 2015

DOI: 10.1007/s10854-014-2421-1

5 authors, including:

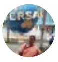

Sinnappan Jesurani
Mother Teresa Women's University
42 PUBLICATIONS **275** CITATIONS
SEE PROFILE

Kanagesan Samikannu
University of Malaya
77 PUBLICATIONS **524** CITATIONS
SEE PROFILE

Ismayadi Ismail
Universiti Putra Malaysia
145 PUBLICATIONS **584** CITATIONS
SEE PROFILE

Rahim Sabbaghizadeh
Universiti Putra Malaysia
15 PUBLICATIONS **43** CITATIONS
SEE PROFILE

Influence of Er on microstructural and dielectric properties of $CaCu_3Ti_4O_{12}$

S. Jesurani, S. Kanagesan, M. Hashim, I. Ismail & R. Sabbaghizadeh

Journal of Materials Science: Materials in Electronics

ISSN 0957-4522

J Mater Sci: Mater Electron
DOI 10.1007/s10854-014-2421-1

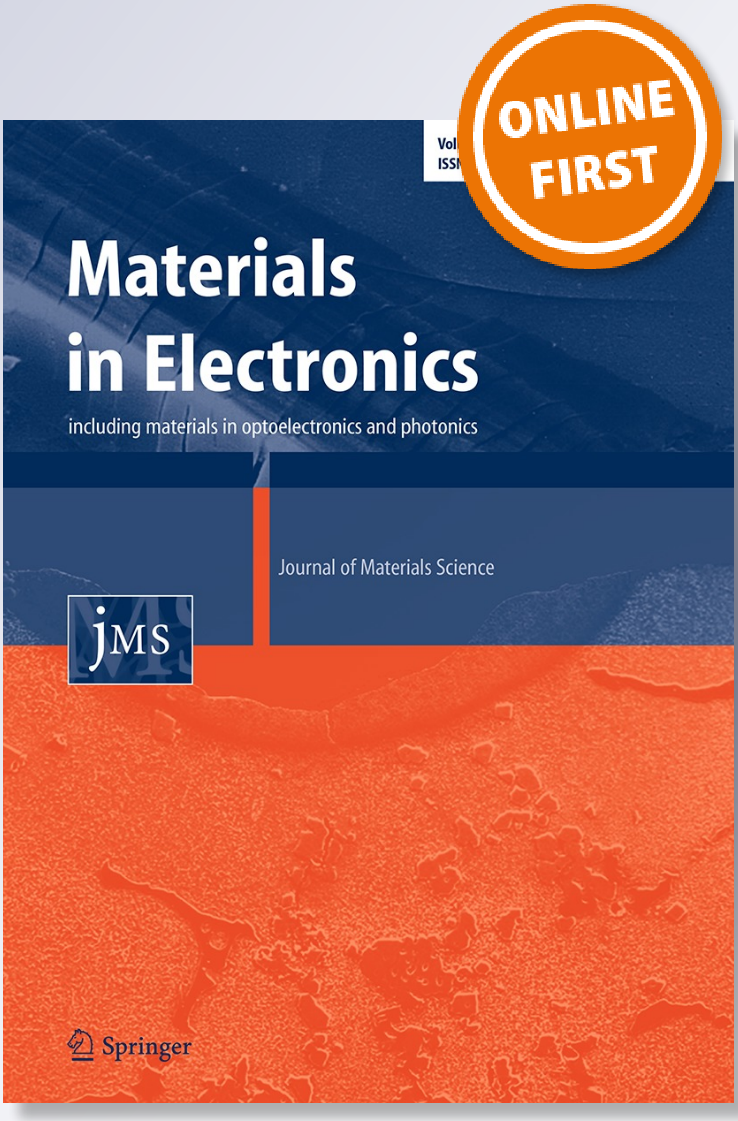

Springer

J Mater Sci: Mater Electron
DOI 10.1007/s10854-014-2421-1

Influence of Er on microstructural and dielectric properties of $CaCu_3Ti_4O_{12}$

S. Jesurani · S. Kanagesan · M. Hashim · I. Ismail · R. Sabbaghizadeh

Received: 22 August 2014 / Accepted: 20 October 2014

Abstract Erbium-doped $CaCu_3Ti_{(4-x)}Er_xO_{12}$ (x = 0, 0.02, 0.1, 0.2, 0.5, 1.0)—(CCTEO) samples were synthesized by using the sol–gel method. The crystal structure did not change on doping with erbium; and it remained cubic when all the six compositions were studied. It was found that lattice parameter increased slightly with Erbium doping. AFM studies showed that the particle size of the CCTEO powder ranged from 52 to 97 nm. The surface morphology of the samples sintered at 1,040 °C in air for 3 h was observed using a high resolution scanning electron microscope. It showed that the grain size was in the range of 0.7–5 μm for these samples. Er doping has been shown to reduce the dielectric loss remarkably while maintaining a high dielectric constant. This result indicates that 0.02 mol% of Er dopant can be used to improve the dielectric properties (dielectric constant- 164,000) of $CaCu_3Ti_4O_{12}$.

1 Introduction

Lead free dielectric materials with high dielectric constant and good thermal stability have attracted increasing attention for their practical applications in cellular phones, global positioning systems, resonators, filters, capacitors and memory devices [1]. There has been a great interest in the synthesis and characterization of a perovskite-type compound, pure and doped calcium copper titanate ($CaCu_3Ti_4O_{12}$), commonly called CCTO [2–8]. CCTO is usually produced by the conventional solid-state reaction from metal oxides at high temperature with several intermediate grindings [9, 10]. Hassini et al. [11] prepared CCTO using an organic gel assisted citrate process and Jha et al. [12] prepared CCTO using a polymeric citrate precursor route but these methods are still complex and require long heat treatment time. Liu et al. [13] prepared CCTO by pyrolyzing an organic solution containing stoichiometric amounts of the metal cations and this was carried out at a lower temperature and a shorter reaction time than the conventional solid-state reaction method. Chen et al. [14] prepared CCTO by the molten salts method. Jin et al. [15] prepared nano CCTO powders using the sol–gel method and the citrate auto-ignition method. Sol–gel synthesis is a well-established low temperature synthesis technique that has recently attracted an increasing amount of interest.

Ceramics based on barium titanate are frequently used in making multilayer capacitors. The rare earth cations, which partly replace the original cation in the spinel structure of barium zirconium titanate, can increase the dielectric properties and prolong the life span of capacitors. Doping titanates with rare earth elements such as Dy, Er and Ho with smaller ionic radii can obtain the centre-shell structure, which is helpful to improve the dielectric properties [16–18]. Earlier researchers on CCTO suggested that intrinsic local dipole moments induced by the Ti displacement could be responsible for the high permittivity as in other high dielectric constant titanates.

S. Jesurani
Department of Physics, Jeyaraj Annapackium College for Women, Periyakulam 625601, Tamil Nadu, India

S. Jesurani
Department of Physics, Center for Material Science and Nano Devices, SRM University, Kattankulathur 603 203, Tamil Nadu, India

S. Kanagesan (✉) · M. Hashim · I. Ismail · R. Sabbaghizadeh
Materials Synthesis and Characterization Laboratory (MSCL), Institute of Advanced Technology (ITMA), Universiti PutraMalaysia, 43400 Serdang, Selangor, Malaysia
e-mail: kanagu1980@gmail.com

We have synthesized Er doped calcium copper titanate using a sol–gel self-combustion method (Er = 0.0, 0.02, 0.1) and the sol–gel method (Er = 0.0, 0.02, 0.1, 0.2, 0.5, 1.0 mol%). The synthesis of Er doped CCTO using the sol–gel self-combustion has been reported elsewhere [19]. Producing high dielectric constant materials synthesized with lower calcination/sintering temperature has become the subject of study for researchers. While some recently published reports concentrate on different synthesis techniques to reduce the processing temperature, other reports focus on substitutions to change the material property. Hwang et al. [20] reported that Erbium has improved the dielectric properties of $BaTiO_3$. But very limited work is reported on the effects of substituting impurity to CCTO to lower the processing temperature [21, 22]. The purpose of the present work is to investigate the effects of Er-substitute (0, 0.02, 0.1, 0.2, 0.5 and 1 mol%) on the structural, morphological and dielectric changes on CCTO ceramics synthesized by the sol–gel route. The sol–gel method is a chemical solution process, which has received considerable attention due to its simplicity and usefulness for obtaining a homogeneous, fine powder. The crystallization/sintering (processing) temperature is very much reduced compared to any conventional preparation method.

2 Synthesis of $CaCu_3Ti_{4-X}$ Er_xO_{12}

$CaCu_3Ti_{(4-x)}Er_xO_{12}$ abbreviated as CCTEO (x = 0, 0.02, 0.1, 0.2, 0.5, 1.0 mol%) powders were prepared by the sol–gel method using Ca $(NO_3)_2{\cdot}4H_2O$, Cu $(NO_3)_2{\cdot}3H_2O$, $Er(NO)_3$ and $C_{12}H_{28}O_4Ti$ as raw materials. The synthesis of CCTEO nano powder flow chart is shown in Fig. 1. Calcium nitrate and copper nitrate were dissolved in ethanol (solution 1). Titanium tetra isoproxide stabilized by acetyl acetone was dissolved in isopropyl alcohol, Erbium nitrate, dissolved in ethanol was mixed with this solution to give solution 2. Solution 1 and solution 2 were mixed in a beaker and stirred continuously using a magnetic stirrer at room temperature. Acetic acid and Citric acid were added slowly into this solution and the temperature was slowly raised to 90 °C to form a gel. The glacial acetic acid and citric acid were used as chelating reagents. The transparent sol with blue color was obtained after stirring and hydrolyzing the mixture solution. When the mixture was concentrated the viscous liquid transformed into a transparent gel. Finally, the gel was dried at 110 °C for 2 days. Subsequently, the dried precursor was calcined at 650 °C and 800 °C for 3 h for crystallization and the milling process was carried out in order to get a nano powder.

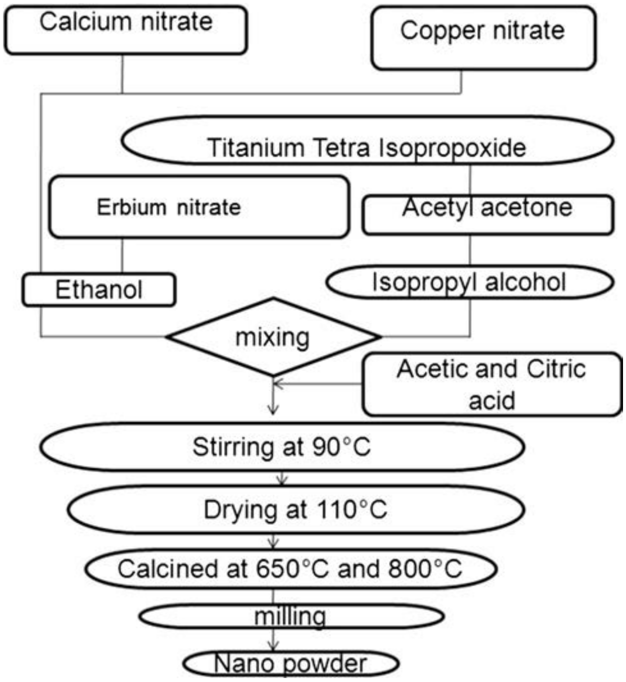

Fig. 1 Flow chart for the synthesis of CCTEO Nanopowder

X-ray powder diffraction (XRD) studies were carried out with an X'PERT-PRO Diffracto meter (Philips, the Netherlands) using Cu Kα1 radiation at 45 kV and 40 mA (λ = 0.154056 nm) in a wide range of 2θ (20° < 2θ < 80°) and particle size measured by Atomic Force Microscopy (AFM) (Agilent 5050/5060). The calcined powder was uniaxially pressed into pellets of 10 mm in diameter and 2 mm in thickness with an applied load of 3.5 tons for 4 min, using polyvinyl alcohol (PVA) as the binder. These pellets were then sintered by using a conventional furnace at 1,020 and 1,040 °C for 4 h. The microstructure of sintered pellets (1,040 °C) was measured by FE-SEM (FEI Quanta 200FEG). The machine also has the analytical capabilities such as detecting the presence of elements down to boron (B) on any solid conducting materials through the energy dispersive X-ray spectrometry (EDX) providing elemental crystalline information. Silver paste was coated over the parallel faces of the pellets and the dielectric constant [23] measurements were made using an LCR meter (Hioki 3532-50) in the frequency range 50 Hz–1 MHz at room temperature.

3 Results and discussion

3.1 X-ray diffraction pattern of calcined $CaCu_3Ti_{4-x}$ Er_xO_{12} powder

Figure 2 shows the X-ray powder diffraction patterns [24] for the system CCTO and $CaCu_3Ti_{(4-x)}Er_xO_{12}$ (x = 0, 0.02, 0.10, 0.20, 0.50 and 1.00) calcined at 800 °C for 3 h. The main peaks of pure CCTO and Er doped CCTO

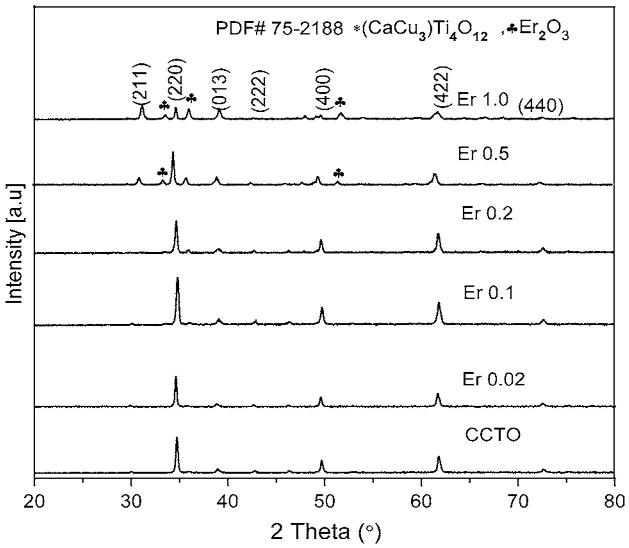

Fig. 2 XRD patterns of CCTO powder calcined in air at 800 °C and $CaCu_3Ti_{(4-x)}Er_xO_{12}$ powder (x = 0, 0.02, 0.10, 0.20, 0.50 and 1.00) calcined at 800 °C for 3 h

powders calcined at 800 °C were compared with the standard powder diffraction pattern (JCPDS card No: 75-2188). The major planes corresponding to (211), (220), (013), (222), (400), (422) and (440) were found to be matched with Cubic $(CaCu_3)\ Ti_4O_{12}$. From the XRD pattern it was found that the concentration of Erbium doped with CCTO was within the limit of its solubility up to x = 0.2 and hence there was no second phase. When x = 0.5 and 1.0, all the main peaks were matched and extra peaks are present which indicates the excess amount of erbium which is not within the limit of its solubility.

The calculated lattice parameters for different values of x are given in Table 1. The lattice parameter increases slightly with the increasing dopant concentration of x = 0.02, 0.1, 0.2 and 0.5. The increase in lattice parameter can be explained in terms of the oxidation state of erbium ion, if it is assumed that erbium exists in trivalent state, Er^{3+}, which has larger a ionic radius [0.881 Å] than the host Ti^{4+} [0.61 Å] ion [25]. The dopant concentration of x = 1.0 slightly decreases the lattice parameter may be due to excess amount of erbium oxide concentration. In the XRD patterns, when x = 1.0 the intensity level of the peaks also decreases. These variations in lattice parameters agree well with the published report [26].

3.2 AFM analysis

Figure 3 shows the AFM images of CCTO powders calcined at 800 °C for different values of x. The crystalline powder was dispersed in acetone and coated on a silicon substrate. The dispersed particles were analyzed using AFM. The shape of the particles was polyhedral and the size of the particle was in the range of 52–97 nm.

Table 1 Crystal system and lattice parameter for CCTEO (x = 0, 0.02, 0.10, 0.20, 0.50 and 1.00)

System	Amount of erbium x	Crystal system	Lattice parameter (Å)
$CaCu_3Ti_{(4-x)}Er_xO_{12}$	0.00	Cubic	7.409 ± 0.001
	0.02	Cubic	7.383 ± 0.001
	0.10	Cubic	7.400 ± 0.001
	0.20	Cubic	7.406 ± 0.001
	0.50	Cubic	7.410 ± 0.001
	1.00	Cubic	7.381 ± 0.001

3.3 FESEM analysis

Figure 4a, b, c, d, e, f shows FE-SEM micrographs (microstructure) [27] of CCTO and CCTEO ceramics sintered at 1,040 °C for 4 h. The grains were equiaxial and the grain sizes ranged from 0.7 to 5 µm. The morphology of the undoped specimen consists of some huge grains, surrounded by small ones. Increasing the concentration level significantly, changed the grain shapes. From Fig. 4a, b, c, d, the grains possess similar shapes and in Fig. 4e, f grain shapes were changed. Jesurani et al. [28] reported an obvious change in grain size and its shape with higher level doping (0.1 mol% and above) in CCTO. From their results, increase in dopant level illustrates pebble to sphere and sheet-like grains, surrounded by blurry grain boundaries which may be caused by the excess liquid composed of oxide phase of dopant during high temperature sintering.

The microstructure showed a matrix consisting of large grains wherein the small grains were embedded between the larger grains. The porosity present in the samples was intergranular in nature, which are not observed in higher concentrations as the grains are highly agglomerated. The grains are found to be a regular and polyhedral type in the lower concentration of Er dopant. The surplus Er ions may merge small crystals at the grain boundaries to become more agglomerated. The precipitated grains will result in grain boundary pinning and impede the growth of the CCTO grains in thick-sheet-like shape for higher concentrations. It is known that the liquid phase is formed during higher concentrations of Er which could assist the densification through particle rearrangement, solution reprecipitation and solid skeleton processes. Thomas et al. [29] reported that dielectric properties of CCTO ceramics have shown a strong dependence on microstructure. The dense microstructure of a sample could lead to excellent electrical properties.

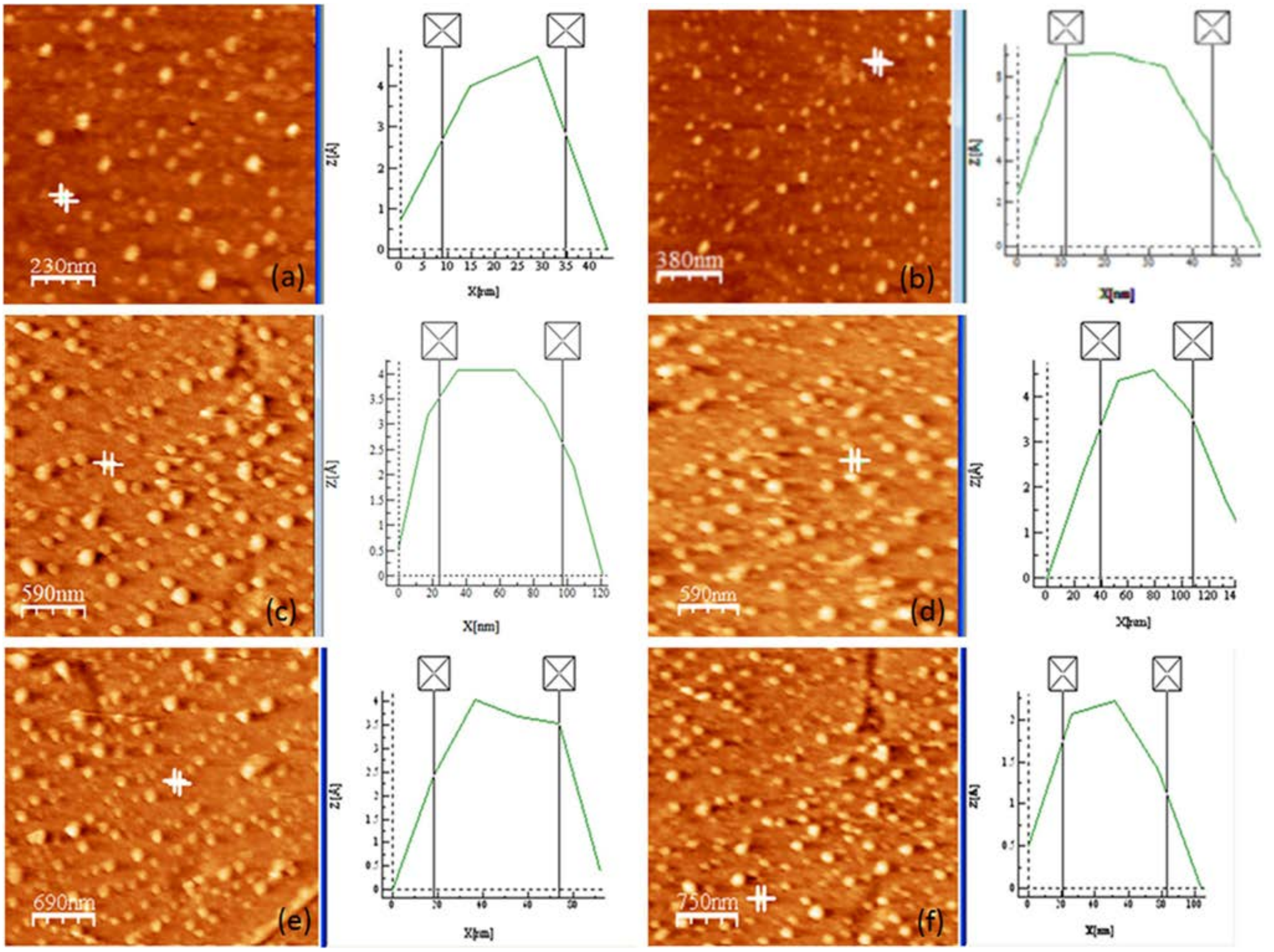

Fig. 3 AFM measurement of Nano powders calcined at 800 °C for 3 h; $CaCu_3Ti_{(4-x)}Er_xO_{12}$ (x = 0, 0.02, 0.10, 0.20, 0.50, and 1.00) (**a–f**)

3.4 EDX analysis

The Energy dispersive X-ray (EDX) spectra for the composition of x = 0.02 (a) and 1.00 (b) are shown in Fig. 5. This spectrum shows the presence of Ca, Cu, Ti and Er as per stoichiometric ratio in CCTEO ceramics. There are reports suggesting that CuO segregates to the grain boundaries even at the stoichiometric composition of (Cu/Ca = 3) [30]. The weight and atomic percentage composition of the constituent elements in CCTEO (x = 0.02 and 1) for grains and grain boundary obtained by energy dispersive X-ray spectrometer (EDX) is shown in Fig. 5a, b. Table 2 shows the weight and atomic percentage of the elements, (x = 0.02 and 1.00).

3.5 Dielectric studies

Figure 6 presents the results of dielectric constants for erbium-doped $CaCu_3Ti_4O_{12}$ sintered at 1,020 and 1,040 °C. The dielectric constant at 50 Hz for samples sintered at 1,020 °C drops from 26,500 for erbium concentration of 0.02 mol% to 8,900 when the concentration of erbium is increased to 0.1 mol% and then again increases to 25,400 for the concentration of 0.20 mol%. However when the sample is sintered at 1,040 °C, a giant dielectric constant of 164,000 is obtained when the concentration of erbium is 0.02 and the corresponding dielectric loss value is 2.0.

The frequency dependence of the dielectric constant and the dielectric loss (tan δ) for CCTO, CCTEO (x = 0.02, 0.10, 0.20, 0.50 and 1.00), at room temperature are shown in Fig. 7. The dielectric constant drops from 26,500 at the frequency of 50 Hz to 1,460 at the frequency of 100 kHz and slightly increases to 3,940 at the frequency 1.0 MHz sintered at 1,020 °C. (a) The dielectric loss drops from 3.3 at the frequency of 50 Hz to 0.1 at frequency of 100 kHz and a very small increase of 0.2 at the frequency of 1.0 MHz sintered at 1,020 °C. (b) The dielectric constant drops from 164,000 at the frequency of 50 Hz to 14,200 at the frequency of 1.0 MHz sintered at 1,040 °C. (c) The

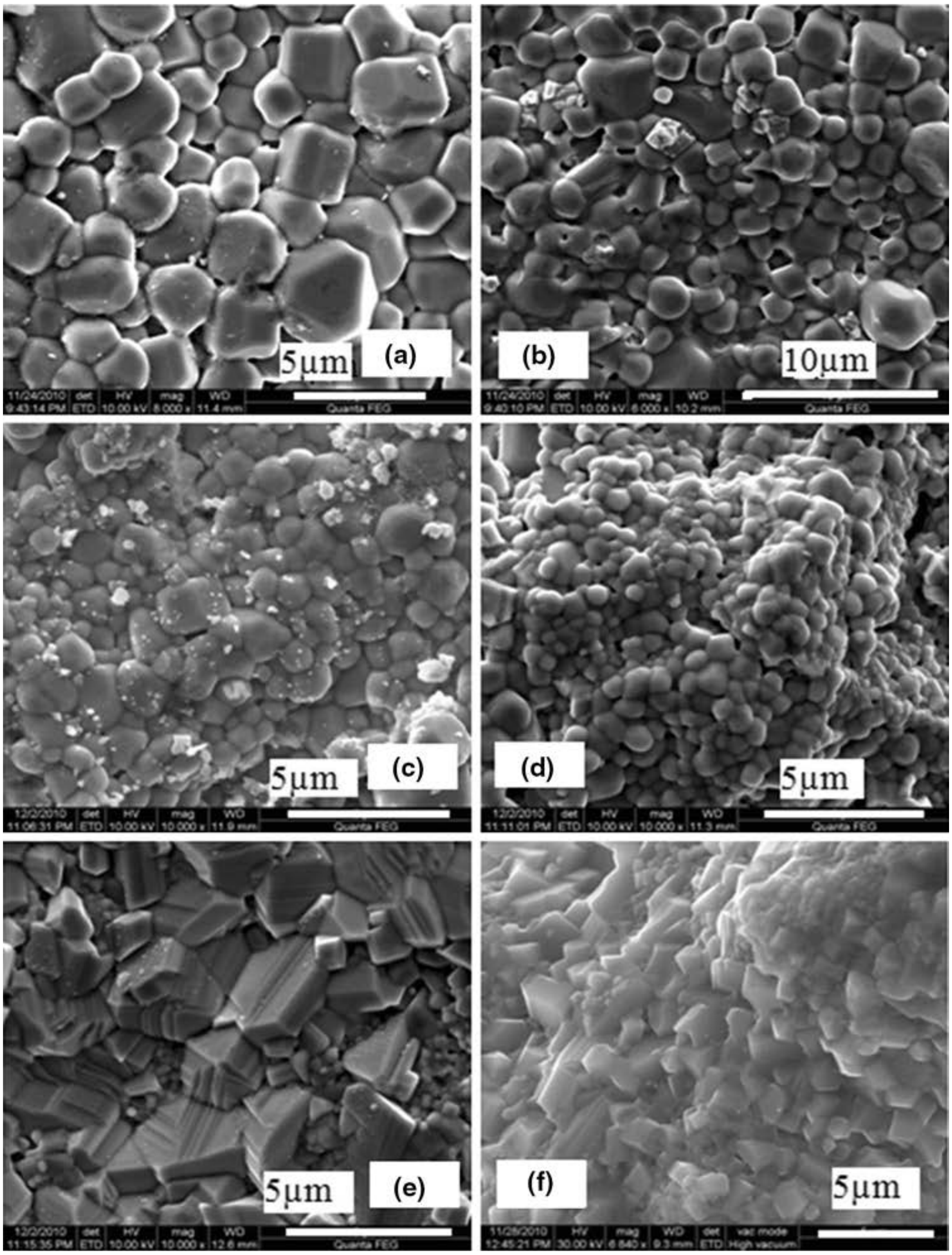

Fig. 4 FE-SEM microstructures of $CaCu_3Ti_{(4-x)}Er_xO_{12}$ with x = 0 **a**, 0.02 **b**, 0.1 **c**, 0.2 **d**, 0.5 **e** and 1.0 **f** ceramics sintered at 1,040 °C for 4 h

dielectric loss drops from 2.0 at the frequency of 50 Hz to 0.1 at the frequency of 100 kHz and the slight increase 1.1 at the frequency of 1.0 MHz sintered at 1,040 °C (d). The dielectric constant of Er doped (x = 0.02) at 1,040 °C sample is 3 times larger than that of pure CCTO (Fig. 7). The high dielectric constant at low frequency [31] region suggests the possibility that the charge carriers accumulate at the interface of semiconducting grains and insulating grain boundaries, which results in interfacial space charge polarization. As the frequency increases, the shift in the maximum dielectric constant shifts towards lower concentration of Er.

This shows that the ceramics obtained possess fine electrical properties. It is noted that the samples are polycrystalline and therefore differ in the relative density of grain boundaries. Such a difference could affect the dielectric constant via the boundary layer mechanism. Electrical heterogeneity originating from the mobile charged species and the internal interfaces in polycrystalline CCTEO gives rise to the polarization in semiconducting grains and insulating grain boundaries [32, 33]. The grain boundary in-homogeneity was confirmed by the existence of electrical potential barriers via current–voltage measurements. So far, the internal barrier layer capacitor

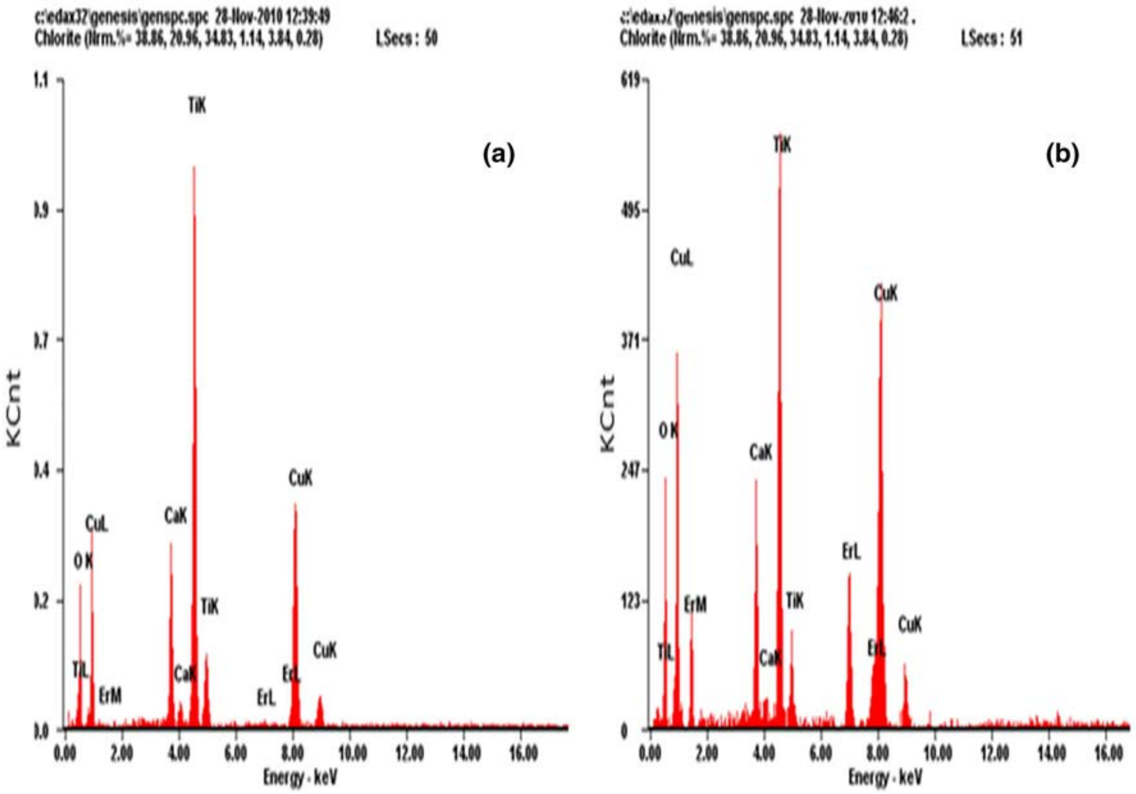

Fig. 5 EDX analysis of CCTEO (x = 0.02 and 1.00) ceramics sintered at 1,040 °C in air for 4 h

Table 2 Weight and atomic percentage of elements for $CaCu_3Ti_{(4-x)}Er_xO_{12}$ for x = 0.02, and 1.00 mol%

Elements	x = 0.02 mol%		x = 1.00 mol%	
	Wt%	At%	Wt%	At%
Ca	5.57	3.95	4.46	3.73
Cu	29.85	13.36	28.23	14.90
Ti	25.55	15.16	15.59	10.91
Er	1.14	0.19	20.03	4.02
O	37.89	67.34	31.70	66.44

(IBLC) model has been widely accepted as the most likely mechanism to elucidate the high dielectric constant in CCTO. The dopant concentration with (x = 0.02, 0.1, 0.2, 0.3, 0.5 mol%) is responsible for high dielectric properties. Extra impurity present in samples synthesized with x = 0.5 and 1.0 mol% gave additional support to improve the dielectric properties.

Choudhury et al. [34] have reported that the dielectric constant of Zr doped $BaTiO_3$ samples prepared by a solid state reaction at a sintering temperature of 1,250 °C showed a maximum value of about 1,000 for 100 kHz. When Zr doped $BaTiO_3$ is synthesized by mechanical

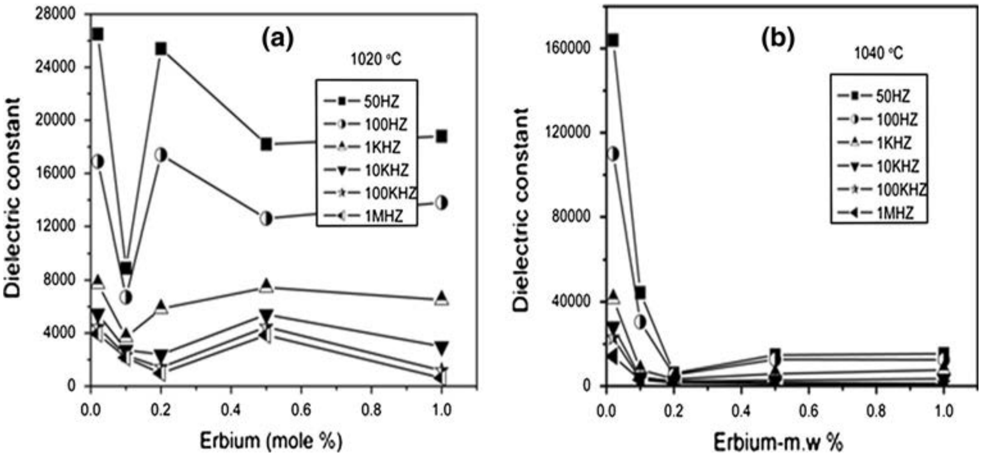

Fig. 6 The dependence of dielectric constant on the concentration of Erbium doped CCTO samples sintered at 1,020 and 1,040 °C Ceramics

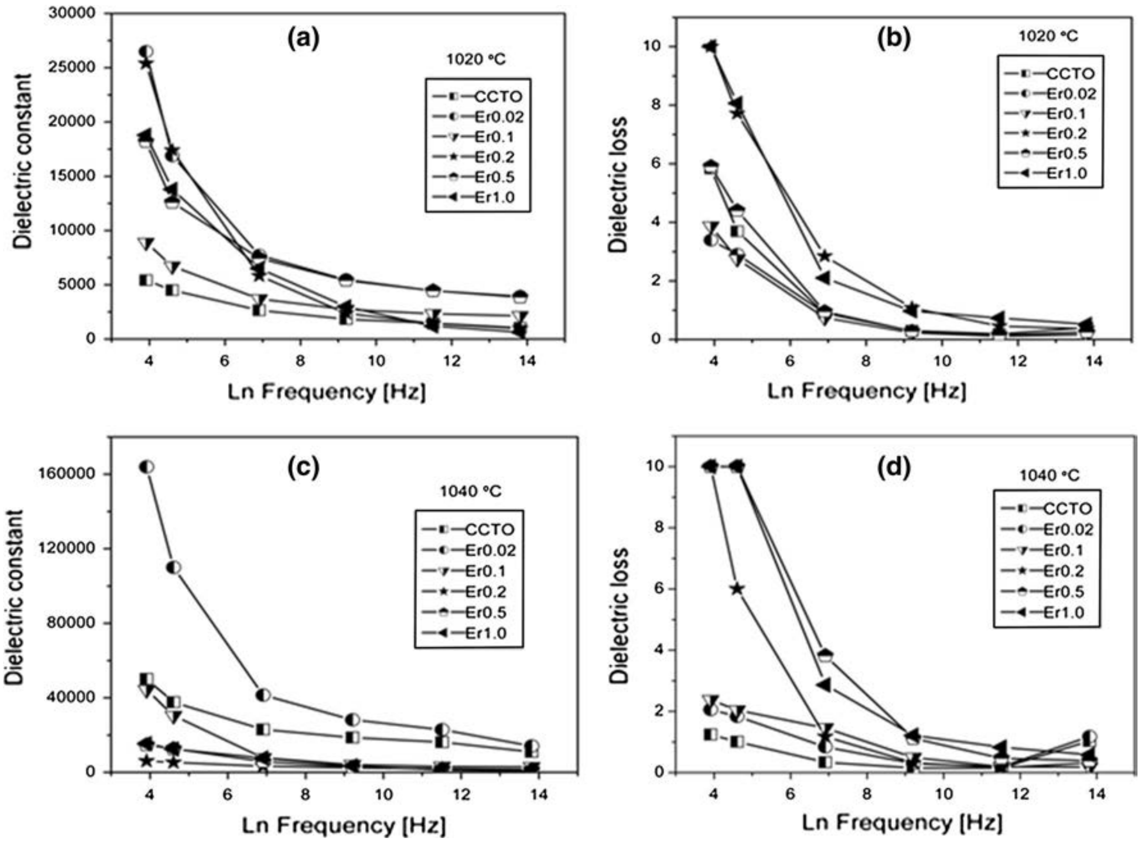

Fig. 7 The variation of room temperature dielectric constant and dielectric loss versus frequency of $CaCu_3Ti_{4-x}Er_xO_{12}$ (x = 0.0, 0.02, 0.10, 0.20, 0.50 and 1.00) sintered at 1,020 and 1,040 °C

alloying [35], its dielectric constant and dielectric loss were reported as 539 and 0.035 respectively; however, when the sample is sintered in the range of 1,200–1,400 °C, as in the present investigation, a much higher dielectric constant (164,000) accompanied by a low dielectric loss (2.0) is obtained. The sintering temperature which is above 1,100 °C [36–39] in the recently published investigations has been brought lower to 1,040 °C in the present work.

4 Conclusion

In summary, a giant-dielectric-constant calcium–copper–zirconium titanate nano powder was successfully synthesized by the sol–gel technique with a lower processing temperature. The CCTEO phase formation was confirmed by the X-ray diffraction pattern. Substitution of rare earth trivalent dopant Er on the Ti site was investigated at various doping concentrations (x = 0.02–1.0). No evidence of secondary phases was observed from XRD analysis. The microstructure study shows that the increasing erbium concentration above x = 0.5 changes the shape of grains; dense microstructure of sample was obtained with good electrical properties. Energy dispersive X-ray spectroscopy for the ceramics (x = 0.02 and 1.0) sintered at 1,040 °C in air for 4 h, confirmed the presence of Erbium. From the results of conventional sintered dielectric measurements, x = 0.02 exhibited a low dielectric loss of around 2.0 with high dielectric constant of 164,000 at 50 Hz.

Acknowledgments We would like to thank SRM UNIVERSITY for providing the Nanotechnology center Facilities and ITMA, UNIVERSITI PUTRA MALAYSIA for the pre-submission final editing of this paper.

References

1. B. Renner, P. Lunkenheimer, M. Schetter, A. Loidl, A. Reller, S.G. Ebbinghaus, J. Appl. Phys. **96**(8), 4400 (2004)
2. A.K. Rai, N.K. Singh, S.K. Acharya, L. Singh, K.D. Mandal, Mater. Sci. Eng. B **177**, 1213 (2012)
3. K.D. Mandal, A.K. Rai, L. Singh, O.M. Parkash, Bull. Mater. Sci. **35**, 433 (2012)
4. A.K. Rai, N.K. Singh, S.-K. Lee, K.D. Mandal, D. Kumar, O. Parkash, J. Alloys. Compd. **509**, 8901 (2011)
5. A.K. Rai, N.K. Singh, S.-K. Lee, K.D. Mandal, D. Kumar, O. Parkash, J Mater Sci: Mater Electron. **22**, 1286 (2011)
6. F. Amaral, M. Valente, L.C. Cost, Mater. Chem. Phys. **124**, 580 (2010)

7. K. Chen, X. Zhang, Ceram. Int. **36**, 1523 (2010)
8. P. Thomas, K. Dwarakanath, K.B.R. Varma, T.R.N. Kutty, J. Therm. Anal. Calorim. **95**, 267 (2009)
9. T.B. Adams, D.C. Sinclair, A.R. West, Adv. Mater. **14**, 1321 (2002)
10. D.C. Sinclair, T.B. Adams, F.D. Morrison, A.R. West, Appl. Phys. Lett. **80**, 2153 (2002)
11. A. Hassini, M. Gervais, J. Coulon, V.T. Phouc, F. Gervais, Mater. Sci. Eng. B **87**(2), 164 (2001)
12. P. Jha, P. Arora, A.K. Ganguli, Mater. Lett. **57**, 2443 (2003)
13. J. Liu, Y. Sui, C. Duan, W.N. Mei, R.W. Smith, J.R. Hardy, Chem. Mater. **18**(16), 3878 (2006)
14. K. Chen, X. Zhang, Ceram. Int. **36**(5), 1523 (2010)
15. S. Jin, H. Xia, Y. Zhang, J. Guo, J. Xu, Mater. Lett. **61**, 1404 (2007)
16. K. Watanabe, H. Ohsato, H. Kishi, Y. Okino, O. Kohzu, Y. Iguchi, T. Okuda, Solid State Ionics **108**(1–4), 129 (1998)
17. B.D. Stojanovic, J. Mater. Process. Technol. **143–144**, 78 (2003)
18. S. Hao, L. Sun, J.X. Huang, Mater. Chem. Phys. **109**, 45 (2008)
19. S. Jesurani, S. Kanagesan, T. Kalaivani, K. Ashok, J. Mater. Sci.: Mater. Electron. **23**, 692 (2012)
20. J.H. Hwang, Y.H. Han, Jpn. J. Appl. Phys. **40**, 676 (2001)
21. A.K. Rai, N.K. Singh, S.K. Acharya, L. Singh, K.D. Mandal, Mater. Sci. Eng. B **177**, 1207 (2012)
22. A.K. Rai, N.K. Singh, S.K. Lee, K.D. Mandal, D. Kumar, O. Parkash, J. Alloys. Compd. **509**, 8901 (2011)
23. R.D. Shannon, C.T. Prewtt, Acta Cryst. B. **1970**, 26 (1046)
24. O. Parkash, D. Kumar, A. Goyal, A. Agrawal, A. Mukherjee, S. Singh, P. Singh, J. Phys. D Appl. Phys. **41**, 035401 (2008)
25. S. Dhanuskodi, A. Philominal, J. Philip, J. Yi, Arch. Appl. Sci. Res. **5**(4), 154 (2013)
26. N.S. Patil, S.K. Bachhav, D.S. Bhavsar, Arch. Appl. Sci. Res. **6**(1), 45 (2014)
27. K.V. Madhale, M.Y. Salunkhe, S.V. Bangale, Arch. Appl. Sci. Res. **5**(1), 62 (2013)
28. S. Jesurani, S. Kanagesan, K. Ashok, J. Sol–Gel. Sci. Technol. **64**(2), 335 (2012)
29. P. Thomas, K. Dwarakanath, K.B.R. Varma, J. Eur. Ceram. Soc. **32**, 1681 (2012)
30. R.D. Shannon, C.T. Prewtt, Acta Cryst. B. **1970**, 26 (1046)
31. D. Anbuselvi, D. Jayaraman, V. Joseph, Arch. Phys. Res. **4**(1), 35 (2013)
32. S. Jesurani, S. Kanagesan, R. Velmurugan, C. Thirupathi, M. Sivakumar, T. Kalaivani, Mater. Lett. **65**, 3305 (2011)
33. S. Aygun, X. Tan, J.-P. Maria, D.P. Cann, J. Electron. Ceram. **15**, 203 (2005)
34. S. Choudhury, S. Akter, M.J. Rahman, A.H. Bhuiyan, S.N. Rahman, N. Khatun, M.T. Hossain, J. Bangladesh Acad. Sci. **32**, 221 (2008)
35. C. Gomez-Yanez, E. Cruz-Aquino, J.J. Cruz-Rivera, R. Linares-Miranda, J. Alloys. Compd. **434–435**, 806 (2007)
36. M. Li, X.L. Chen, D.F. Zhang, W.Y. Wang, W.J. Wang, Sens Actuators B **147**, 447 (2010)
37. W. Makcharoen, J. Tontrakoon, G. Rujijanagul, D.P. Cann, T. Tunkasiri, Ceram. Int. **38**, S65 (2012)
38. P. Thomas, K. Dwarakanath, K.B.R. Varma, J. Eur. Ceram. Soc. **32**, 1681 (2012)
39. J.J. Romero, P. Leret, F. Rubio-Marcos, A. Quesada, J.F. Fernandez, J. Eur. Ceram. Soc. **30**, 737 (2010)